Increased Lateral Abutment Resistance from Gravel Backfills of Limited Width

Interim Report on Load Tests Performed for
Work Task 3

by

Kyle M. Rollins, Ku Hyon Kwon and Travis M. Gerber

Department of Civil and Environmental Engineering

Brigham Young University
368 CB Provo, Utah 84602

Prepared for

Utah Dept of Transportation Research Division
Lead Agency for Pooled-Fund Study
"Dynamic Passive Pressure on Abutments and Pile Caps"

May 2008

Increased Lateral Abutment Resistance from Gravel Backfills of Limited Width

Kyle M. Rollins, M. ASCE [1]; Ku Hyun Kwon[2]; and Travis M. Gerber, M. ASCE [3]

ABSTRACT: Lateral pile cap tests were performed on a pile cap with three backfills to evaluate the static and dynamic behavior. One backfill consisted of loose silty sand while the other two consisted of dense gravel zones 0.91- and 1.82-m wide between the pile cap and the loose silty sand. The 0.91- and 1.82-m wide dense gravel zones increased the lateral resistance by 75 to 150% and 150 to 225%, respectively, relative to the loose silty sand backfill. Despite being thin relative to the overall shear length, the 0.92- and 1.82-m wide gravel zones increase lateral resistance to 59% and 83%, respectively, of the resistance that would be provided by a backfill entirely composed of dense gravel. The dynamic stiffness for the pile cap with the gravel zone decreased about 10% after 15 cycles of loading, while the damping ratio remained relatively constant with cycling. Dynamic stiffness increased by about 10 to 40% at higher deflections, while the damping ratio decreased from an initial value of about 0.30 to around 0.26 at higher deflections.

Keywords: passive pressure; pile caps; gravel; load test; dynamic response

INTRODUCTION

Numerical analyses conducted by several investigators indicate that the passive force-deflection relationship for bridge abutments plays a significant role in the seismic response of bridges. For example, in parametric analyses of a bridge using a 3D finite element model, Faraji

[1] Prof., Civ. & Env. Engrg. Dept., Brigham Young University, 368 CB, Provo, UT 84602; rollinsk@byu.edu.
[2] Staff Engr., GeoEngineers, Inc., 523E 2nd Ave, Spokane, WA 99202; kkwon@geoengineers.com
[3] Asst. Prof., Civ. & Env. Engrg. Dept., Brigham Young University, 368 CB, Provo, UT 84602, tgerber@byu.edu

et al. (2001) found that switching from a loose to a dense abutment backfill substantially decreased bridge deflection and reduced pile head moment by a factor of two. In addition, the stiffer response produced a two-fold increase in axial force and bending moment in the bridge deck. Analyses conducted by El-Gamal and Siddharthan et al. (1998) as well as Shamshabadi et al. (2007) also indicate significant influences of abutment stiffness on bridge response.

Several large-scale tests have demonstrated that the passive force contributed by dense gravel backfills can provide lateral resistance comparable to that provided by the piles in a pile cap or abutment (Rollins and Sparks 2002; Mokwa and Duncan 2001, and Rollins and Cole 2006). However, in many locations gravel is expensive and would not be commonly used for approach fills. In such cases it may prove cost-effective to compact a thin zone of gravel adjacent to an abutment wall. This approach would be comparable to placing compacted gravel fill below a spread footing. For a spread footing, bearing capacity can be significantly improved if the fill thickness is equal to the width of the footing (Hanna and Meyerhof, 1980). In the case of an abutment wall, most of the lateral passive force is developed within a depth of 2 to 2.5 m (Martin et al. 1996) where deflections are sufficient to mobilize passive force even though the entire abutment wall may be 5 to 8 m high. These observations suggest that a gravel zone extending 2 m deep and only 1 to 2 m behind an abutment wall might develop a significant percentage of the lateral passive force which would develop if the entire backfill consisted of dense gravel. The lateral resistance provided by a thin gravel zone may also be important when a limited width of compacted gravel is placed around a pile cap, as specified by some state departments of transportation.

To investigate the effect of a thin, dense gravel zone on lateral passive resistance, large-scale lateral load tests were performed on a pile cap with and without backfill on one side. In

one test, the backfill consisted of loose silty sand, while in two subsequent tests the backfill consisted of dense gravel zones 0.91-m and then 1.82-m wide immediately adjacent to the pile cap with the same loose silty sand beyond the gravel. Load was applied incrementally using a deflection control approach to define the static load-deflection curve. Most previous large-scale passive force tests have only been conducted statically. In the absence of dynamic test data, engineers have often used equivalent static analyses and neglected the effects of cyclic loading or increased resistance provided by damping in many seismic investigations. To help define dynamic stiffness and damping values as a function of cyclic loading, 15 cycles of loading were also applied dynamically after each static deflection increment.

TEST LAYOUT

Plan and profile views of the overall layout for the passive load tests are shown in Fig. 1. The main test feature was a pile cap against which backfill was compacted. Two hydraulic actuators were also used to apply both the static and cyclic loads to the test pile cap as shown in Fig. 1. The actuators reacted against an even larger pile cap. The same 5.18m × 3.05m × 1.12m concrete pile cap constructed previously by Rollins et al (2003) and used by Rollins and Cole (2006) was also used for this field test series. The pile cap was constructed of reinforced concrete with a compressive strength of about 34.5 MPa (5000 psi) while the top and bottom mats of horizontal reinforcing steel consisted of No.25 bars (soft metric) at 150 mm spacing in the long direction and No. 29 bars at 300 mm spacing in the short direction. The pile cap was supported by twelve 324-mm (12.75-in) OD steel pipe piles with a 9.5-mm thick pipe wall which were filled with concrete. The piles were connected to the pile cap by a reinforcing cage which consisted of six No. 25 bars with No. 13 hoops spaced at 305 mm. The reinforcing cage

extended to a depth of 1.7 m into the piles and 1.06 m above the piles to tie into the upper reinforcing mat in the pile cap. The piles were driven closed-ended approximately 12.2 m (40 ft) into the soil profile in a 4 × 3 configuration with 1.42 m and 1.06 m (4.4 and 3.3 pile diameter) center-to-center spacing in the long and short direction under the pile cap. Adjacent to the pile cap was a reaction foundation that was supported by nine steel pipe piles driven open-ended in a 3 × 3 configuration to a depth of about 12.2 m (40 ft). The steel pipe piles had an outside diameter of 610 mm (24-in) and a wall thickness of 12.7 mm.

The lateral load was applied to the test pile cap by two 2.7 MN (600 kip) MTS hydraulic load actuators situated between the test and reaction pile caps. In order to apply the cyclic lateral load, the end of each actuator was attached to the vertical face of each pile cap at a height of 0.36 m above the base of each pile cap. Sixteen 50-mm diameter high strength threaded bars (four bars for each end of actuators) were used to connect the actuators to the two pile caps.

Testing Procedure and Testing Sequence

The lateral load testing was performed using a deflection control approach. The actuators applied equal load to each side of the pile cap until a specified target deflection was obtained. This deflection was then held constant for about a minute while manual readings were obtained. Thereafter, 15 deflection-controlled bi-directional cycles were applied with a frequency of about 1 Hz and an amplitude of about ± 2.5 mm. At the completion of the cyclic loading, the actuators increased the load until the next target deflection was achieved and the procedure was repeated. Target deflection levels were 6.35, 12.7, 19.05, 25.4, 31.75, 38.1, 44.45, 50.8, and 63.5 mm.

Four lateral load tests were performed on the pile cap as illustrated schematically in Fig. 1. Initially, a lateral load test was performed without any backfill in place to provide a "baseline" force-deflection relationship for the pile cap itself. Because the pile cap had been

previously loaded a number of times (Rollins and Cole 2006), the baseline force-deflection curve is known to be relatively linear. Subsequently, a lateral load test was performed with the backfill consisting entirely of loose silty sand. Vertically, the sand backfill adjacent to the front face of the pile cap extended from the top of the cap to 0.3 m below the bottom of pile cap; the backfill was placed below the base of the cap because the log-spiral theory indicates that the failure surface should extend below the base. Horizontally, all the backfills extended 4.9 m (16 ft) in front of the cap and approximately 1.8 m (6 ft) beyond the edge of the cap on each side. Next, lateral load tests were performed after compacting dense sandy gravel zones 0.91 m- and 1.82 m-wide between the pile cap and the loose silty sand which remained in place from the edge of the gravel to a distance of 4.9 m in front of the cap as shown in Fig. 1.

Subsurface and Backfill Characteristics

The silty sand material classified as SM and A-4 according to the Unified Soil Classification and the AASHTO Classification Systems, respectively. The maximum particle size of the fill was 12.5mm with approximately 90% passing the No. 40 sieve and 45% non-plastic fines. The coefficient of uniformity (C_u) and curvature (C_c) were 14.8 and 2.8, respectively. The specific gravity was 2.68. The standard and modified Proctor maximum unit weights were 16.90 and 17.75 kN/m^3, respectively.

The gravel fill was a typical roadbase material which classified as silty, clayey gravel with sand (GC-GM), and A-1-b according to the USCS and AASHTO methods, respectively. The fill had a maximum particle size of 19 mm. C_u and C_c were 454 and 1.2, respectively. The plasticity index (PI) and liquid limit (LL) were 6% and 23%, respectively. The specific gravity was 2.70. The standard and modified Proctor unit weights were 20.06 and 21.68 kN/m^3, respectively.

The dense gravel was compacted in 100 mm-thick lifts using hand-operated compaction equipment to meet Utah DOT backfill specifications which require a minimum unit weight greater than 92% of the modified Proctor maximum unit weight (ASTM D 1577) with an average unit weight greater than 96% of the Proctor maximum unit weight. Nuclear density tests were performed on each layer of compacted gravel fill. All tests indicated a relative compaction (R_c) greater than 92% and the average relative compaction was 97% which is greater than the required average. This average dry unit weight corresponds to a relative density of about 85% according to correlations developed by Lee and Singh (1971). The loose silty sand was also compacted in 100 mm-thick lifts but with much lower energy. The minimum relative compaction was 84% with an average of 88% of the modified Proctor maximum. This corresponds to a relative density of 40% (Lee and Singh 1971). In-situ direct shear tests performed on the dense gravel and loose silty sand backfills indicated that the friction angles for these two materials were 42.6º and 27.7º, respectively. Table 1 provides a summary of grain size distribution and other soil properties for the two backfill soils.

Instrumentation

Applied load was measured by the actuators which were located at a point approximately of 0.56 m below the top of the pile cap, which was near the center of the pile cap. The pile cap deflection was measured using four string potentiometers located on the corners of the back face of the pile cap which were attached to an independent reference frame. Deflection measurements at the top and bottom of the cap were used to determine pile cap rotation.

Pressure at the backfill soil-cap interface was measured using four earth pressure cells and two flexible, thin-film tactile pressure sensors. The 230 mm-diameter stainless steel earth pressure cells were designed with a reinforced backplate to reduce point loading effects when

directly mounting the cell to a concrete or steel structure. The earth pressure cells were mounted flush on the front face of the pile cap. This was accomplished by chiseling four 290-mm (11.5 in) diameter recesses into the face of the pile cap, resurfacing the roughened surface with cement grout, and attaching the cells to the prepared surface with grout and embedded anchors. A vertical groove was cut from the pressure cell location to the top of the cap to accommodate the stem and wiring of the pressure cells. To further protect the pressure cells, a small steel pipe was cut in half lengthwise and placed over the stems which protruded minimally from the cap face.

The flexible thin-film tactile pressure sensors, manufactured by Tekscan, measure pressures on a grid with 10.2 mm spacing in two directions over a 490 mm high and 530 mm wide area. The sensors were calibrated before testing using a bladder system. The thin film sensors were evenly spaced vertically along the height of the pile cap. To help increase compliance at the backfill-sensor-pile cap interface as well as mitigate potential effects of point loading by individual gravel aggregates, a 13-mm veneer of medium dense silty sand was placed between the gravel backfill and the front of the sensors. Proprietary data acquisition software allowed pressures measured across the sensors to be viewed in real-time during testing.

To supplement the electronic instrumentation, a 0.6-m square grid was painted on the top of the backfill prior to load testing. The elevation of each grid point was measured before and after testing to evaluate heave and settlement. In addition, the development of crack patterns in the backfill with increasing static deflection level was mapped using this grid.

TEST RESULTS

Static Load Tests

Plots of the total force, baseline force (no-backfill case), and passive force as a function

of deflection are presented in Fig. 2 for the test with the 1.82-m wide gravel zone. As indicated previously, the baseline force versus deflection curve is relatively linear due to previous lateral load testing. During previous testing, gapping of soil around the piles and beneath the cap had occurred, as well as cracking of concrete at the pile-cap connection. As a result, the lateral load resistance of the cap during this testing had been reduced from its initial load-deflection response, with the remaining lateral resistance due primarily to the structural resistance of the piles themselves. The passive force versus deflection curve was obtained by subtracting the baseline force from the total force at each deflection level. This same approach was used to evaluate the passive force for all of the backfill conditions tested.

Rotation of the cap about a vertical axis did not exceed 0.05º which indicates that the two actuator arrangement was deflecting the cap uniformly. In addition, rotation of the cap about a horizontal axis did not exceed 0.24º for either gravel backfill test. Although this rotation is certainly greater than the 0º rotation assumed for a truly "fixed-head" condition, the rotation is nevertheless relatively small.

Passive Force Versus Deflection

The peak passive force versus deflection curves are plotted in Fig. 3 for the pile cap tests involving both the loose silty sand backfill as well as the 0.91-m and 1.82-m wide dense gravel zones between the pile cap and the loose silty sand backfill. Even though the gravel zone is relatively narrow in comparison to the expected length of the shear zone (≈2.8 m), the placement of the dense gravel zone had a pronounced effect on the mobilized passive force. With the 0.91-m wide gravel zone in place, the passive force was 75 to 150% higher than with the silty sand backfill at any given deflection. With the 1.82-m wide gravel zone in place, the passive force was 150 to 225% higher than with the silty sand backfill. In addition to providing increased

lateral capacity, the 0.91-m wide gravel zone increased the initial loading stiffness by 125% (based on a deflection on the order of 6 mm). In contrast, the 1.82-m wide gravel zone increased the initial loading stiffness by 250%.

Using the spreadsheet program PYCAP developed by Duncan and Mokwa (2001), passive force versus deflection curves were also computed for the pile cap with backfills consisting entirely of loose silty sand and dense gravel. In PYCAP the ultimate passive force is computed using the log-spiral method and the force versus deflection curve is based on a hyperbolic relationship that is dependent on the initial elastic modulus of the backfill soil. The parameters used in making these computations are summarized in Table 2. The friction angles are based on field and laboratory test results, while the initial elastic moduli are based on values suggested by Duncan and Mokwa (2001). The computed passive force versus deflection curves are also plotted in Fig. 3 for comparison purposes. The computed curve for the loose silty sand backfill is in very good agreement with the measured curve. The computed curve for the dense gravel backfill is clearly higher than the measured curves at a given deflection. Nevertheless, placement of the 0.91- and 1.82-m wide gravel zones produced 59% and 83%, respectively of the ultimate resistance expected from a backfill consisting entirely of dense gravel**.** These results clearly indicate the value of placing a thin, but dense, gravel layer adjacent to a pile cap or an abutment wall when increased lateral resistance is desired, but the cost of using large quantities of select backfill material must be minimized.

Passive Soil Pressure Versus Depth

Passive soil pressure versus depth curves obtained from the earth pressure cells on the front face of the pile cap for the two tests involving dense gravel zones are presented in Fig. 4. Individual curves represent conditions immediately after each deflection increment had been

reached. The curves do not generally indicate the traditional triangular distribution. As shown in Fig. 4, measured pressures were generally greatest near the base of the pile cap, but pressures were also higher near the ground surface than at mid-depth. At deflection increments of 19 mm or less, greater passive pressures were mobilized in the thicker of the two gravel backfills. In the case of the 1.82-m wide gravel zone, as the deflection increment exceeded 19 mm, the pattern of the soil pressure distribution changed, with the uppermost pressures continuing to increase with increasing deflection while the lowermost pressures began to decrease with increasing deflection. This behavior is indicative of a rotation behavior once a certain pressure threshold had been exceeded.

Despite the presence of a silty sand veneer between the gravel backfill and the flexible tactile sensors, the flexible tactile sensors experienced significant point loading and damage from the gravel aggregates. Consequently, no meaningful pressure measurements could be extracted from the tactile pressure sensor data for these tests.

The earth pressures measured by the pressure cells were multiplied by the tributary areas associated with each pressure to determine the passive force as a function of deflection. Fig. 5 provides a comparison between the passive force obtained from the four earth pressure cells and the actuator force (minus the baseline response) for the three backfill load tests. The two curve types are generally similar in shape, with the cell-based forces being generally 20% lower for the partial width gravel backfills and somewhat higher for the loose silty sand backfill. A number of individuals have noted the difficulty of obtaining representative pressures from earth pressure cells under all load conditions (e.g., Weiler and Kulhawy 1982, Dunnicliff 1988). Systemic differences may be attributable, in part, to differing pressure conditions outside the spatial coverage provided by the pressure cells. For example, stress concentrations might be expected at

the edges of the pile cap wall which would not be registered by the load cells closer to the center of the wall. The degree of stress concentration at the edge would be affected by the pile cap geometry, soil stiffness and the rigidity of the pile cap. In his elastic analysis of a uniformly loaded strip foundation, for example, Borowicka (1938) determined that the distribution of contact pressure near the centerline could approach 67% of average distributed load applied by the foundation.

Failure Crack Patterns

Plan view drawings showing the crack patterns for the pile cap tests involving the loose silty sand backfill along with the backfills with 0.91- and 1.82-m wide gravel zones are provided in Fig. 6. The crack patterns in Fig. 6 show shear bands extending outward from the edges of each pile cap and semi-circular arcs at the back edge of the failure mass. For the caps with gravel zones, the shear bands extend outward at a wider angle than in the loose sand which increases the effective width of the pile cap which, in turn, increases the passive resistance. Because of the wider effective width, the stress levels on the interface between the dense gravel and the silty sand are much lower than those at the interface between the pile cap and the gravel zone. In addition, the stress level is also likely reduced due to the contrast in stiffness provided by the dense gravel relative to the loose silty sand as is illustrated by elastic solutions for vertical loads on two-layer systems (see Fox 1948).

Level surveys indicate that the entire failure mass tended to heave upward during lateral loading of the loose silty sand backfill. In contrast, the dense gravel zones moved downward about 10 to 15 mm during loading while the loose sand behind it remained at the same elevation or heaved upward at greater distances from the interface (Rollins, Gerber and Kwon, 2007). These observations suggest a rotational failure pattern behind the pile cap.

Dynamic Load Tests

Fig. 7 provides the peak static load-deflection curve for the test with the 0.91-m wide gravel zone. In addition, the load-deflection curves for the 1st and 15th cycles at each deflection increment are also shown. As discussed previously, after the peak static resistance was reached at each deflection increment the deflection was held constant for about one minute after which 15 cycles were applied. During this time interval, creep relaxation in the soil led to a reduction in lateral resistance which ranged from 5 and 18%. As a result, the cyclic load-deflection curves are generally associated with re-loading rather than virgin loading. Therefore, the peak-to-peak secant stiffness of the load-deflection loops is higher than the stiffness of the static curve. Although not shown, the behavior for the test with the 1.82-m wide gravel zone was similar.

A comparison of the 1st and 15th cycle load-deflection loops in Fig. 7 indicates that there is some decrease in the stiffness with cycling; however, the area within the loop appears to remain about the same with cycling. To investigate these observations further, the stiffness and damping ratio were computed for each cycle of loading at each deflection increment. The stiffness, k, was computed using the equation

$$k = \Delta F / \Delta u \tag{1}$$

where ΔF is the change in load and Δu is the change in deflection for the peak points on each cycle. The damping ratio, β, was computed using the equation

$$\beta = \frac{A_{loop}}{2\pi k u^2} \tag{2}$$

where A_{loop} is the area within the load-deflection loop and u is the single amplitude deflection value with respect to the center of the loop for a given cycle.

Plots of the dynamic stiffness and damping ratio as a function of the number of cycles at each deflection increment are provided in Figs. 8 and 9 for tests involving the 0.91-m wide and 1.81-m wide gravel zones, respectively. Apart from the cyclic loading at zero deflection, the stiffness values generally plot within a fairly narrow range for each test. For example, the dynamic stiffness for the test with the 0.91-m wide gravel zone was between 180 and 240 kN/mm, while the dynamic stiffness for the 1.82-m wide gravel zone increased to between 240 and 330 kN/mm. Doubling the width of the gravel zone generally increased the dynamic stiffness by about 35%. For a given static deflection increment the dynamic stiffness decreased very gradually with the number of cycles. After 15 cycles, the stiffness was only 8 to 15% lower than the stiffness for the first cycle.

Apart from the cyclic loading at zero deflection, the computed damping ratios typically plot within a narrow range from 0.26 to 0.30. There is no consistent trend in the damping ratio with the number of cycles and for practical purposes the damping ratio remains essentially constant with cycling.

Fig. 10 provides summary plots of the average dynamic stiffness and damping ratios for the two tests involving gravel zones as a function of deflection. The stiffness and damping ratios are the averages from all 15 cycles at each deflection increment. Initially, the dynamic stiffness increases with deflection for both backfills, but then with further deflection the stiffness decreases for the test with the 0.91-m wide gravel zone and plateaus for the test with the 1.82-m wide gravel zone. Based on the observed crack patterns, the decrease or plateau in stiffness corresponds to the deflection at which the shear bands move through the gravel zones and into the loose sand backfill. With additional deflection, the shear bands extend further into the sand backfill and the dynamic stiffness begins to increase again. This increased stiffness would be

expected due to contraction of the loose sand around the shear zone with continued deflection. Therefore, in contrast to the static loading where the stiffness tends to decrease with increasing deflection (or load) level, the dynamic stiffness is highest at the largest deflections although the increase is only 10 to 20%. A comparison of the two stiffness plots shows that increasing the width of the gravel zone by 0.91 m led to average increases in dynamic stiffness of 30 to 40%.

The damping ratio from the cyclic load-deflection loops tended to decrease somewhat as the initial deflection level (or load level) increased. For example, the damping ratio was typically about 0.30 at low deflection levels and decreased to about 0.26 at the higher deflection levels. There was relatively little difference between the damping ratios for the two different gravel zone thicknesses. In order for the damping ratio to remain constant while the stiffness increases, the damping force must also increase in proportion to the square root of the increase in stiffness.

CONCLUSIONS

Based on the results of the field testing and analysis of the test data the following conclusions can be drawn.

1. Placement of a relatively thin, but dense, gravel backfill zone between a pile cap or abutment wall and a loose silty sand backfill can significantly increase the static passive force provided by the backfill. Specifically, in these tests with a 5.2-m long, 1.12-m high concrete face, a 0.91-m wide gravel zone increased the passive force by 75 to 150% relative to the loose silty sand backfill alone, while a 1.82-m wide gravel zone increased the passive force by 150 to 225%.
2. In addition to providing increased lateral capacity, a 0.91-m wide gravel zone increased the initial loading stiffness by 125% relative to the loose silty sand backfill alone, while a 1.82-m wide gravel zone increased the initial loading stiffness by 250%.
3. A thin dense gravel zone in front of loose sand can also produce a significant percentage of the lateral passive resistance that would obtain if the entire backfill consisted of dense gravel. For example, in these tests, gravel zones 0.91- and 1.82-m wide in front of loose silty sand produced passive resistance that was 59% and 83%, respectively, of that predicted for the backfill consisting entirely of dense gravel.
4. Based on the crack patterns, the wide angle of the shear planes in the dense gravel zone spread the passive pressure over a much greater area than the width of the pile cap. As a result, the stress levels on the interface between the dense gravel and the silty sand are much lower than those at the interface between the pile cap and the gravel zone. In addition, the stress level is also likely reduced due to the contrast in stiffness provided by the dense gravel relative to the loose silty sand.

5. The dynamic stiffness of the backfill with compacted gravel zones showed a relatively small decrease (approx. 8 to 15%) after 15 cycles of loading at a given initial deflection level, whereas the damping ratio remained relatively constant after 15 load cycles.
6. Increasing the thickness of the dense gravel layer increased the dynamic stiffness of the backfill. The dynamic stiffness of the 1.82-m wide gravel zone was 30 to 40% higher than that for the 0.91-m wide gravel zone.
7. The dynamic stiffness initially increased with deflection until the shear bands extended through the gravel zones. As the shear zones moved into the loose sand, the dynamic stiffness decreased or remained constant, but at even greater deflections where contraction of the soil would have occurred during shearing, there was an increase in the dynamic stiffness of 10 to 40% at the maximum deflection for the 0.91- and 1.82-m wide zones, respectively.
8. The average damping ratio from the cyclic load-deflection loops tended to decrease somewhat as the initial deflection level (or load level) increased. For example, the damping ratio was typically about 0.30 at low deflection levels and decreased to about 0.26 at the higher deflection levels.
9. Although the damping force increased for the backfill with a 1.82-m wide gravel zone relative to that with a 0.91-m wide gravel zone, the damping ratio versus deflection curves remained essentially the same for both cases. This suggests that the increase in damping force was proportional to the square root of the increase in stiffness.

ACKNOWLEDGMENTS

This research investigation was supported by the National Science Foundation under

Award Number CMS-0421312, the George E. Brown, Jr. Network for Earthquake Engineering Simulation (NEES) which operates under NSF Award Number CMS-0402490, and the Departments of Transportation from the states of California, New York, Montana, Oregon and Utah through an FHWA pooled-fund arrangement. This support is greatly appreciated. The Utah Dept. of Transportation served as the lead agency for the pooled-fund study with Daniel Hsiao as the Project Manager. The conclusions and recommendations expressed in this paper are those of the authors and do not necessarily reflect the views of the sponsors.

REFERENCES

Borowicka, H. (1938). "Distribution of pressure under a uniformly loaded elastic strip resisting on elastic-isotropic ground." *2nd Cong. Int. Assoc. Bridge Struct. Engrg.* Vol. 8 (3).

Duncan, J.M. and Mokwa, R. L. (2001). "Passive earth pressures: theories and tests." *J. Geotechnical and Geoenv. Engrg.,* ASCE, Vol. 127 (3), 248-257.

Dunnicliff, J. (1988). *Geotechnical Instrumentation for Monitoring Field and Performance.* Wiley, New York, 577 p.

El-Gamal, M. and Siddharthan, R.V. (1998). "Stiffness of Abutments of Piles in Seismic Bridge Analyses." *Soils and Foundations*, Japanese Geotechnical Society, Vol. 38 (1), 77-87.

Faraji, S. Ting, J.M., Crovo, D.S., and Ernst, H. (2001). "Nonlinear analysis of integral bridges; finite-element model." *J. Geotechnical & Geoenviron. Engrg*., ASCE, Vol. 127 (5), 454-461.

Fox, L. (1948). "Computations of traffic stresses in a simple road structure". *Proc. 2nd Int. Conf. on Soil Mech. and Found. Engrg*. Vol. 2, 236-246.

Hanna, A.M. and Meyerhof, G.G. (1980). "Design charts for ultimate bearing capacity of foundations on sand overlying soft clay," *Can. Geotech. J.*, Vol. 17 (2), 300-303.

Lee, K.W. and Singh, A. (1971). "Relative Density and Relative Compaction." *J. Soil Mech. And Found. Div*., ASCE, Vol. 84 (SM2), 1654-1 to 1654-35.

Martin, G. R., Lam, I. P., Yan, L.-P., Kapuskar, M., and Law, H. (1996). "Bridge abutments—Modeling for seismic response analysis." *Proc., 4th CALTRANS Seismic Research Workshop*, California Department of Transportation, Sacramento, CA, 15 p.

Mokwa, R. L. and, Duncan, J. M., (2001). "Experimental evaluation of lateral-load resistance of pile caps." *J. Geotechnical and Geoenv. Engrg.,* ASCE, Vol. 127 (2), 185-192.

Rollins, K. M. and Cole, R. T., (2006). "Cyclic Lateral Load Behavior of a Pile Cap and Backfill" *J. Geotechnical & Geoenv. Engrg.*, ASCE, Vol. 132 (9), 1143-1153.

Rollins, K.M. and Sparks, A.E. (2002) "Lateral Load Capacity of a Full-Scale Fixed-Head Pile Group." *J. Geotechnical and Geoenv. Engrg.,* ASCE, Vol. 128 (9), 711-723.

Shamshabadi, A., Rollins, K.M., Kapaskur, M. (2007). "Nonlinear Soil-Abutment-Bridge Structure Interaction for Seismic Performance-Based Design." *J Geotechnical and Geoenv*., ASCE, Vol. 133 (6), 707-720.

Weiler, W.A. and Kulhawy, F.H. (1982). "Factors affecting stress cell measurements in soil." *J. of the Geotech. Eng. Div.,* ASCE, Vol. 108 (GT12): 1529-1548.

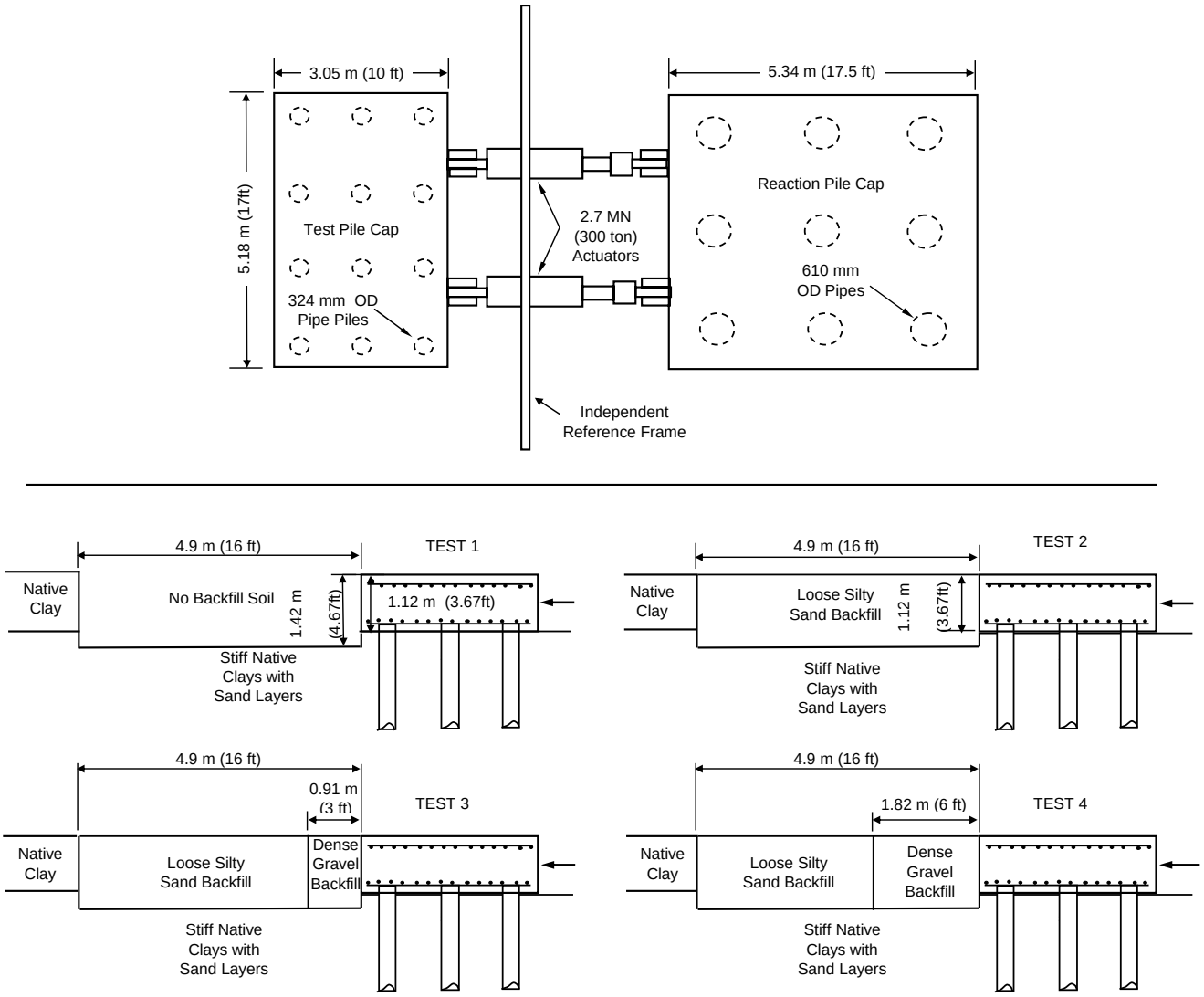

Fig. 1. Plan and profile views of the test layout for the large-scale passive force tests.

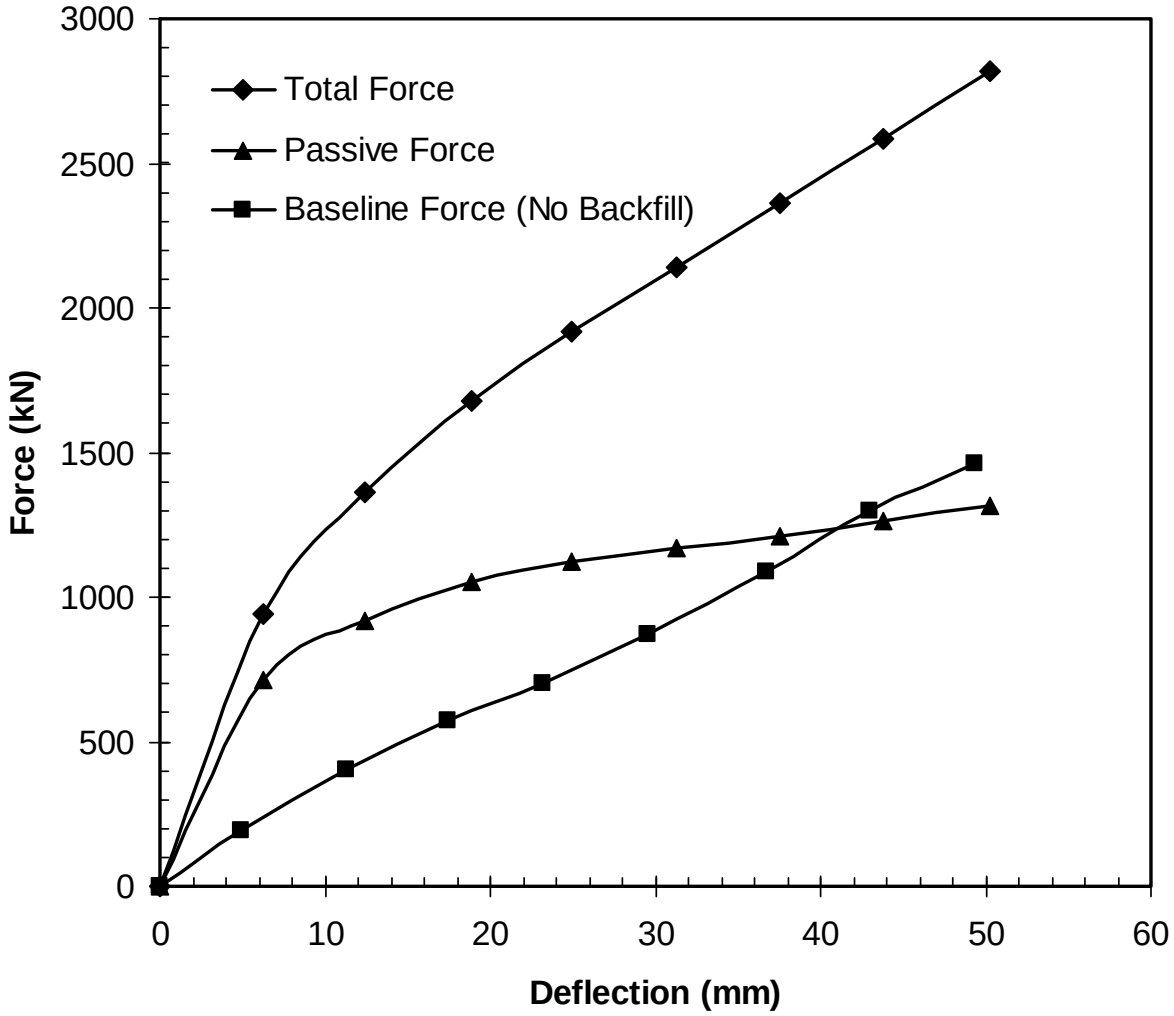

Fig. 2. Plots of total force, baseline force, and passive force vs. deflection for the pile cap with backfill consisting of a 1.82-m wide zone of dense sand in front of loose silty sand.

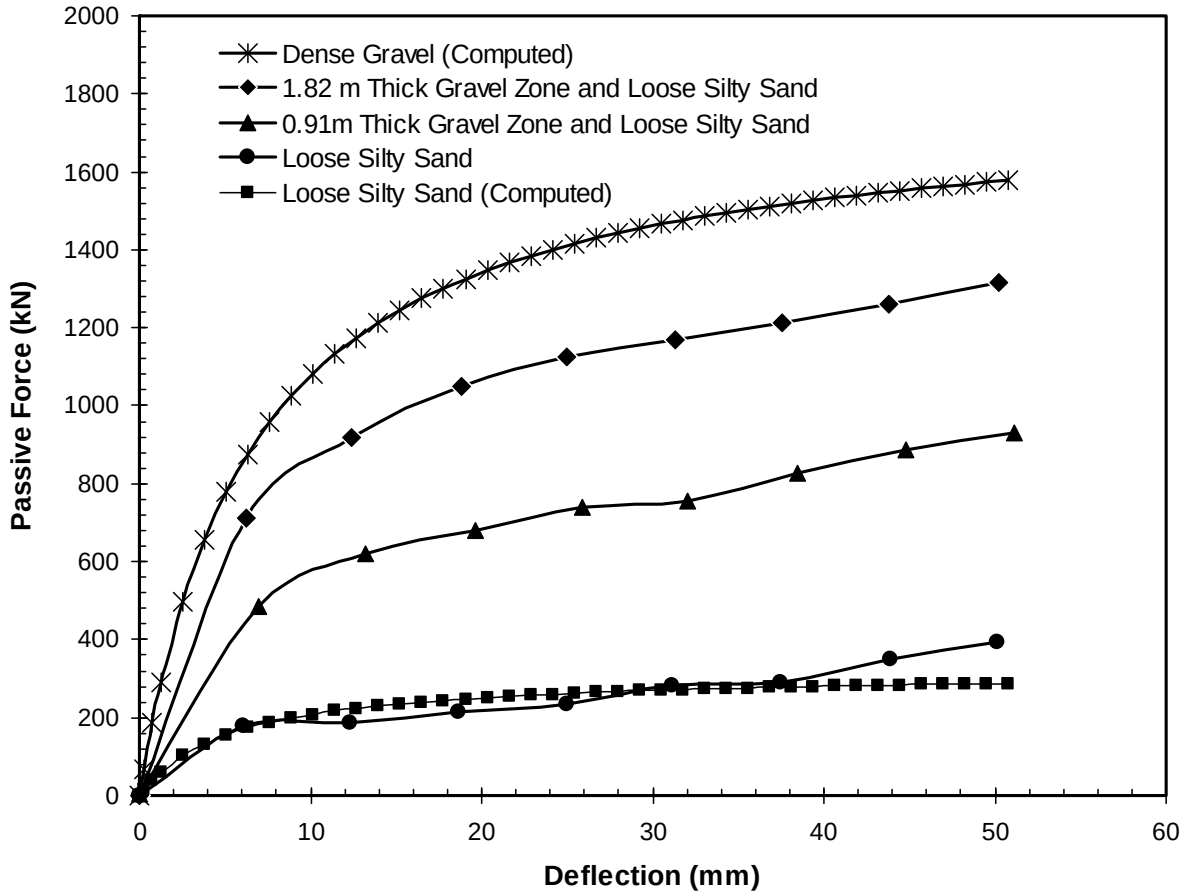

Fig. 3. Measured passive force vs. deflection curves for a pile cap with loose silty sand backfill and with 0.91- and 1.82-m wide dense gravel zones with loose silty sand backfill. Computed curves for backfills entirely of loose silty sand and dense gravel are also shown.

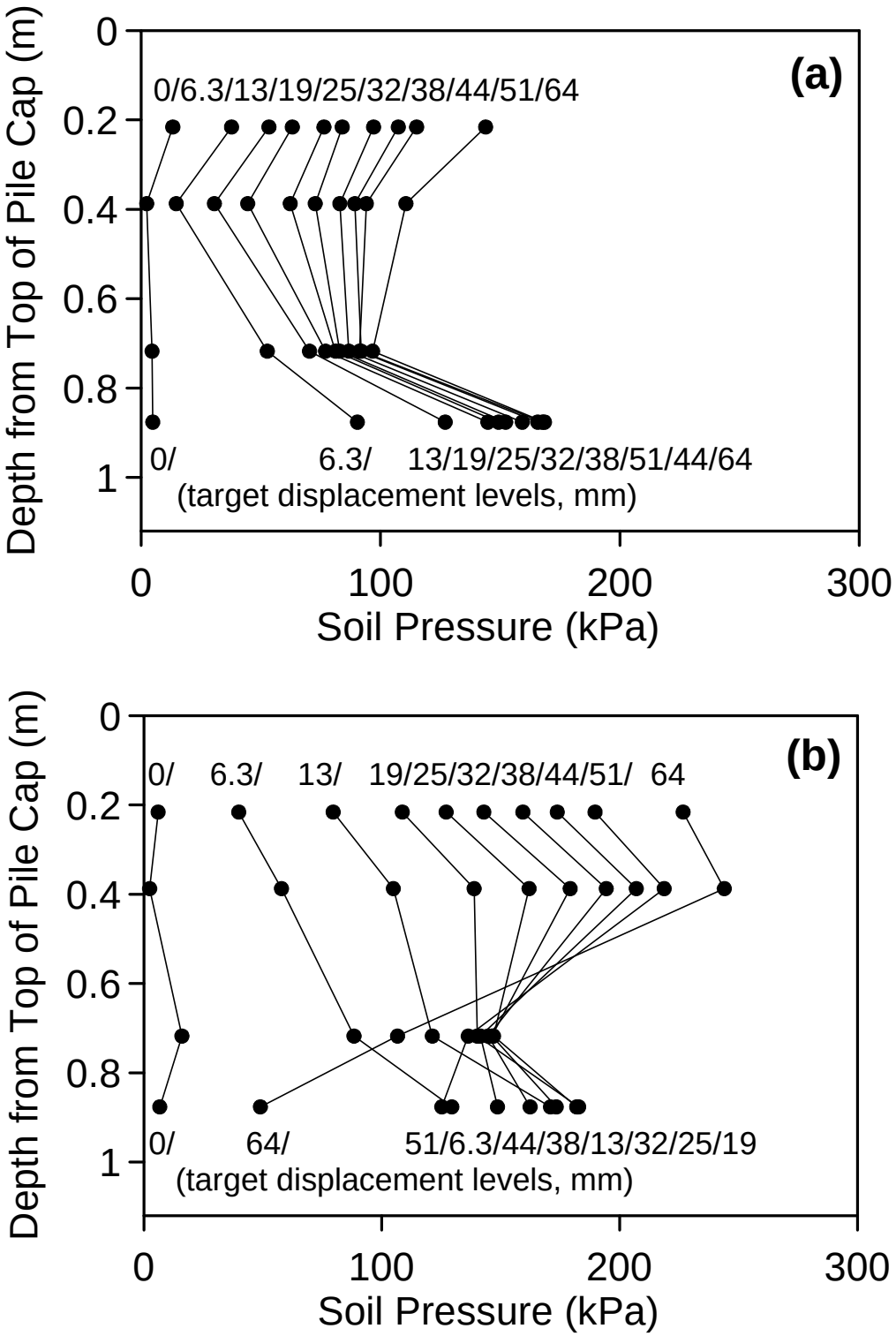

Fig. 4. Pressure vs. depth curves at various deflection increments for the backfill with (a) the 0.91-m wide gravel zone and (b) the 1.82-m wide gravel zone.

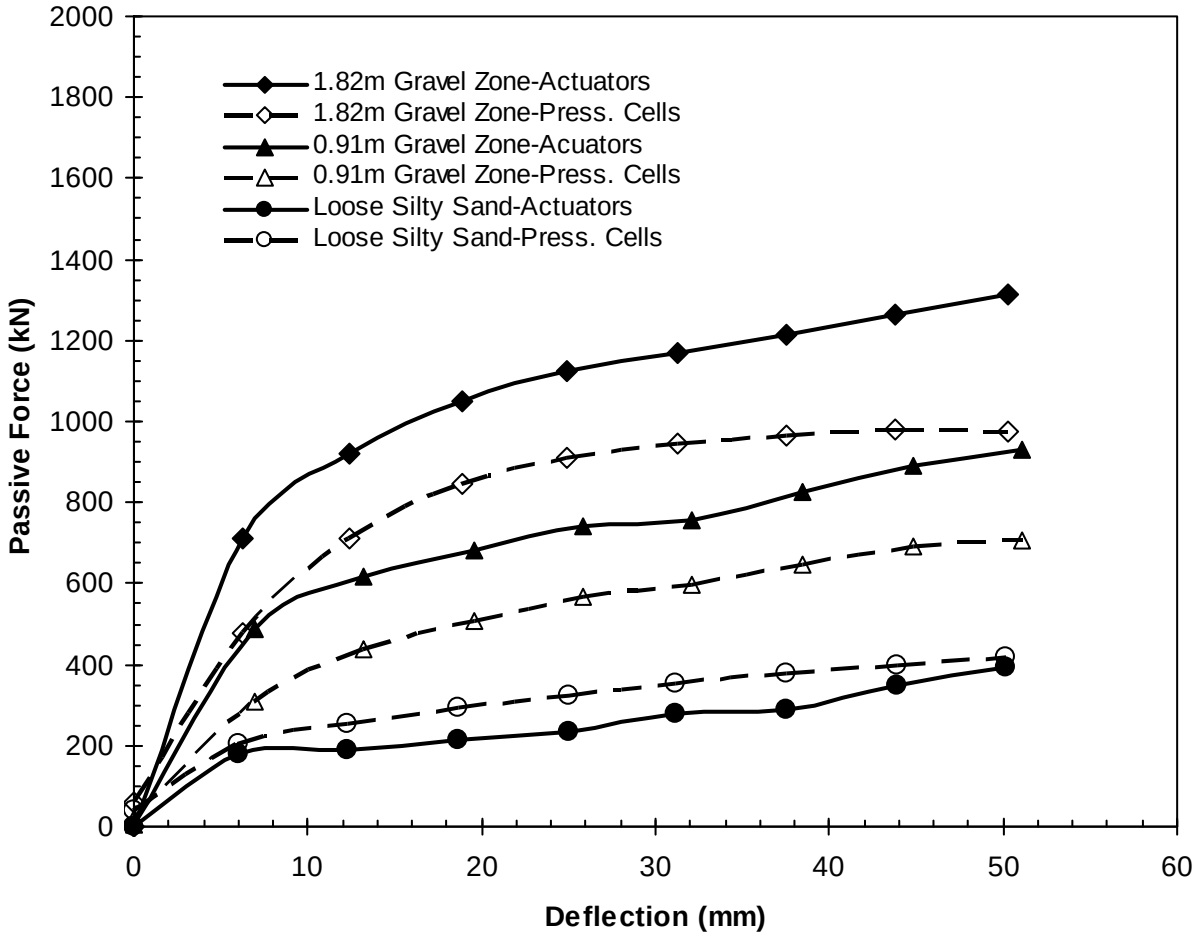

Fig. 5. Comparison of passive force vs. deflection curves obtained from hydraulic actuators and earth pressure cells for lateral pile cap tests.

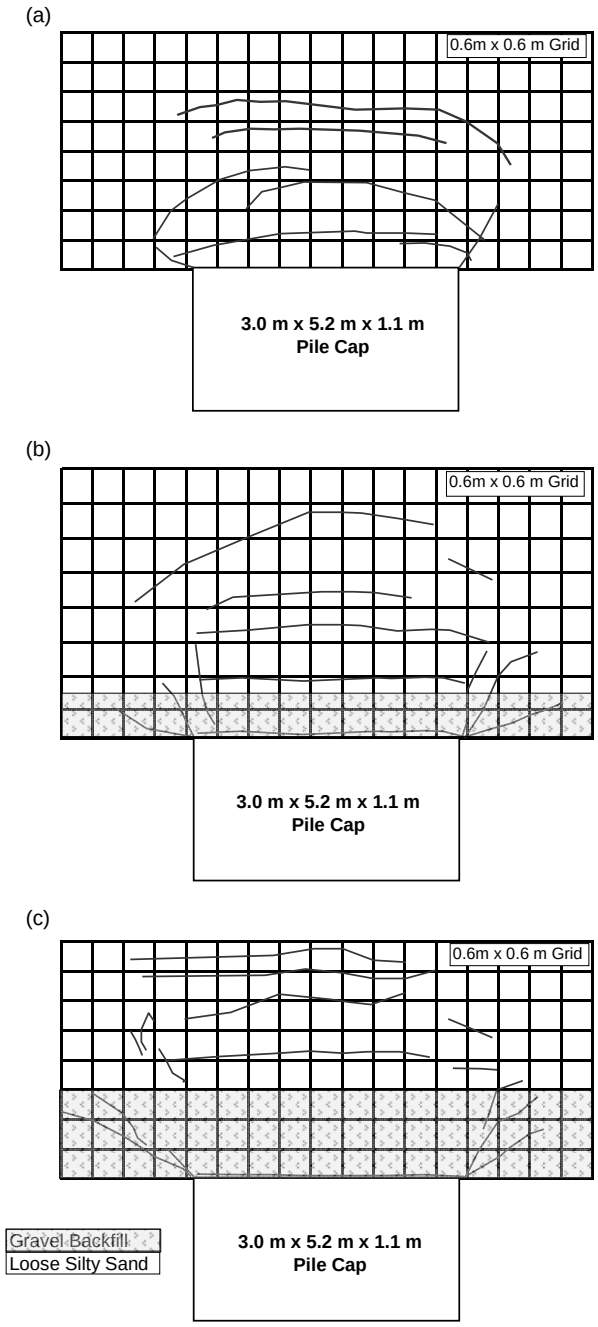

Fig. 6. Plan view of crack patterns with backfills consisting of (a) loose silty sand, (b) 0.91-m wide dense gravel zone with loose silty sand, and (c) 1.82-m wide dense gravel and loose silty sand.

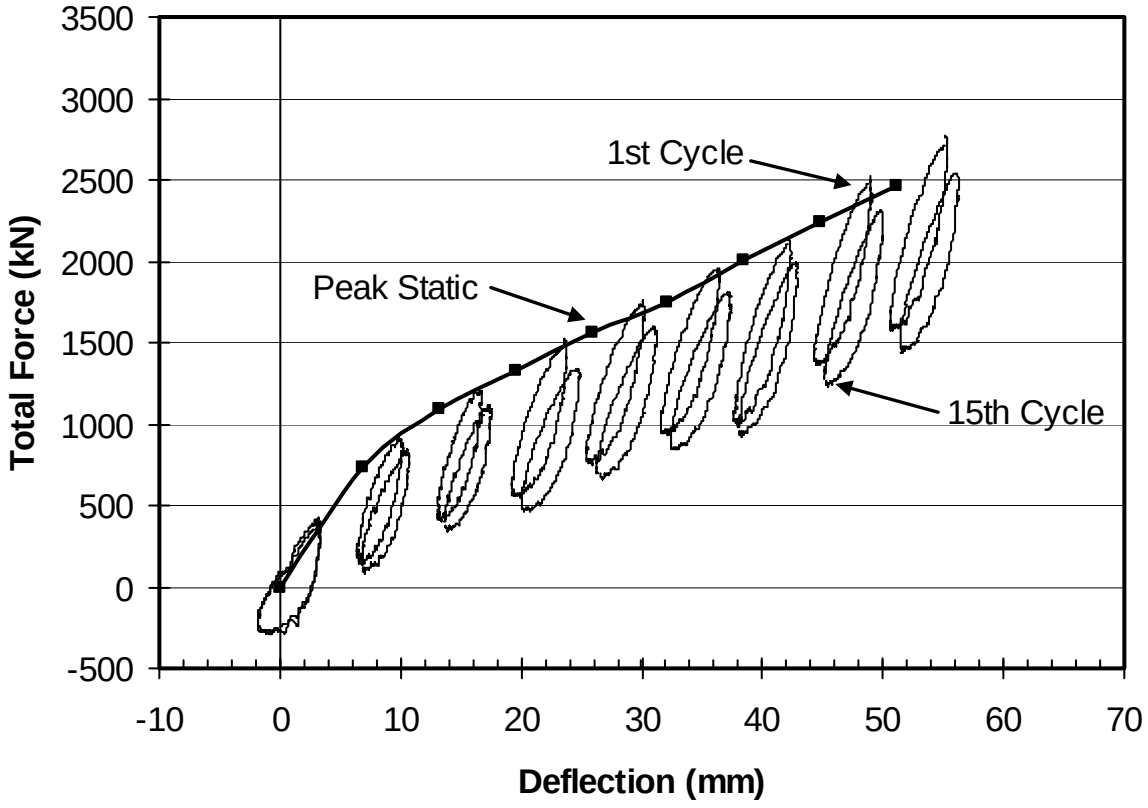

Fig. 7. Plots of peak static load-deflection along with 1st and 15th load cycles at each deflection increment for tests involving 0.91-m wide gravel zone.

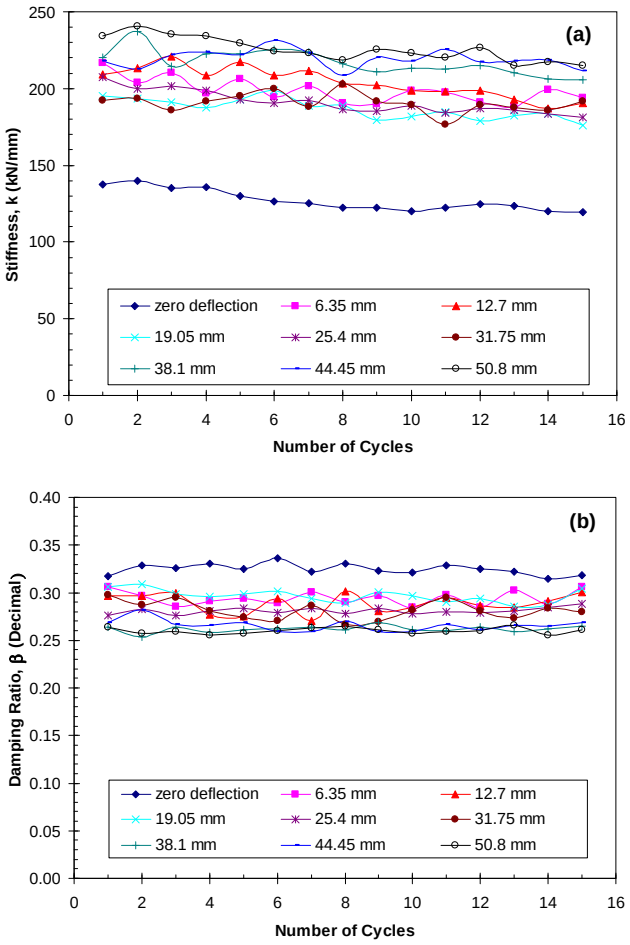

Fig. 8. Plots of (a) dynamic stiffness and (b) damping ratio as a function of number of cycles at each initial deflection increment for the pile cap with a 0.91-m wide dense gravel zone.

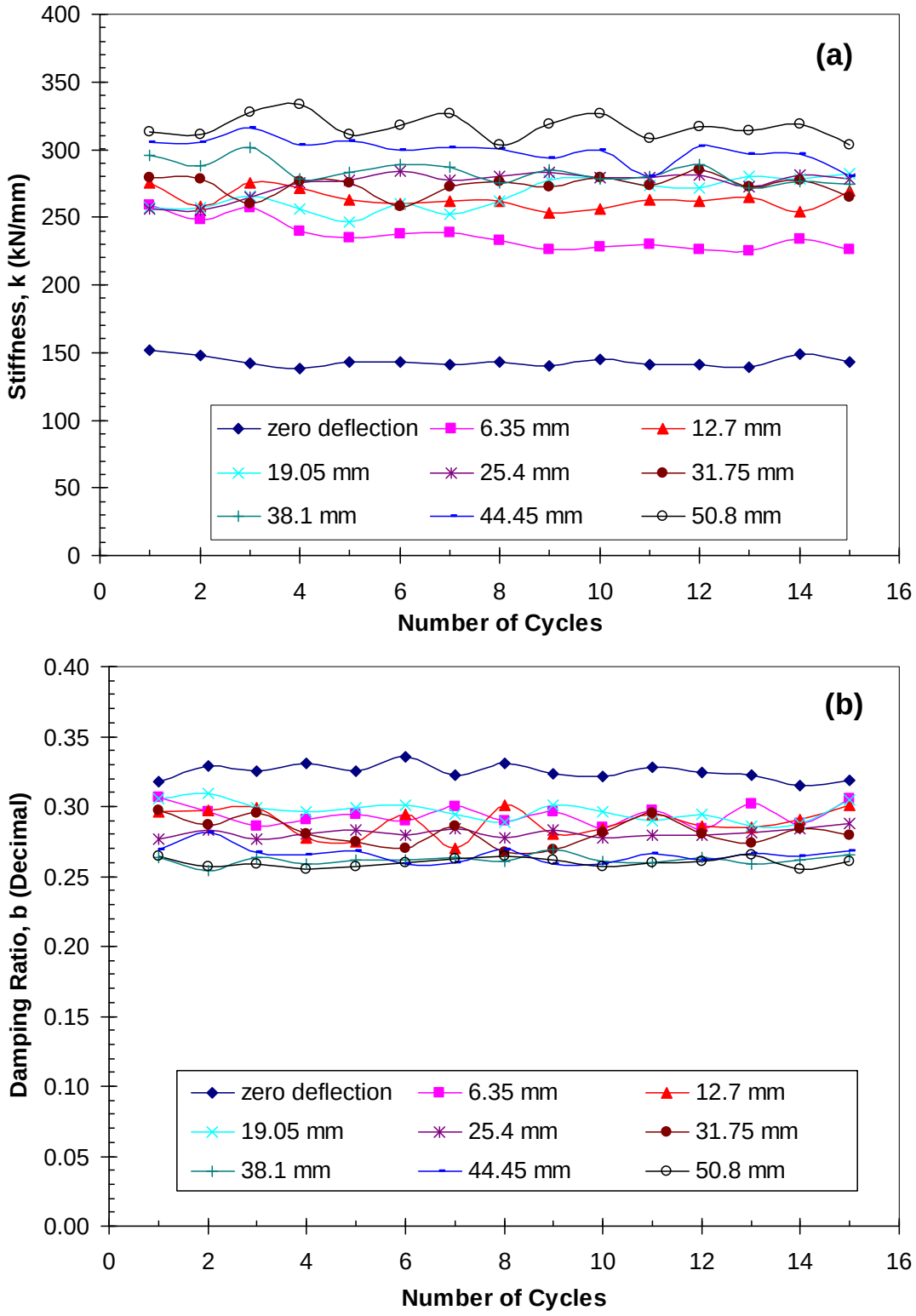

Fig. 9. Plots of (a) dynamic stiffness and (b) damping ratio as a function of number of cycles at each initial deflection increment for the pile cap with a 1.82-m wide dense gravel zone.

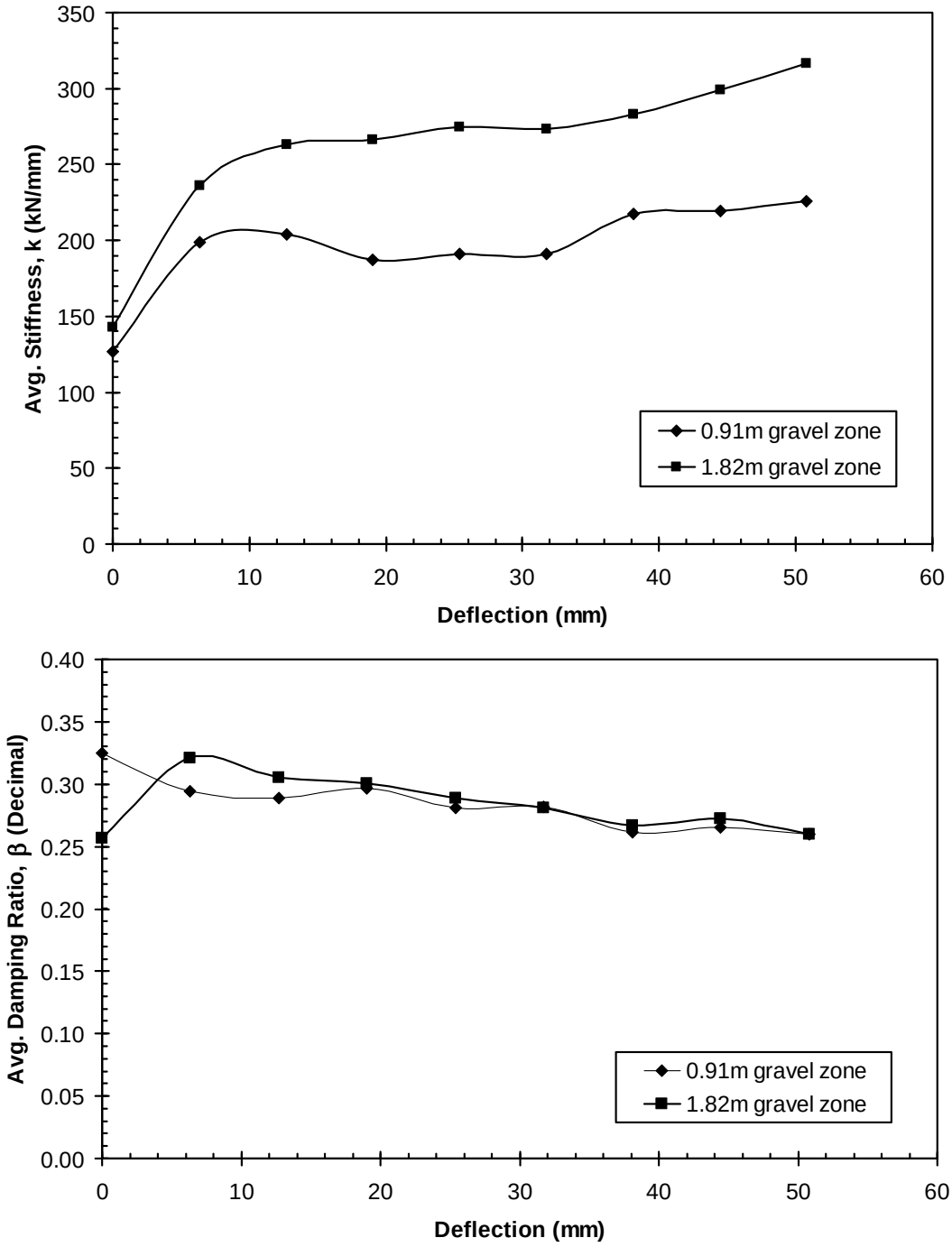

Fig. 10. Plots of (a) average dynamic stiffness and (b) average damping ratio as a function of deflection level for the backfill tests involving 0.91- and 1.82-m wide dense gravel zones.

Table 1. Summary of Properties of Backfill Materials

Backfill Type	Gravel (%)	Sand (%)	Fines (%)	Modified Proctor w_{opt} (%)	Modified Proctor $(\gamma_d)_{max}$ (kN/m^3)	As Compacted w_{opt} (%)	As Compacted $(\gamma_d)_{max}$ (kN/m^3)	As Compacted R_c (%)	As Compacted D_r (%)	As Compacted ϕ (°)
Silty Sand	2.4	52.9	44.7	11	17.75	11	15.69	88	40	27.7
Gravel	49.7	30.5	19.9	7	21.68	6	20.9	97	85	42.6

Table 2. Summary of Backfill Soil Properties Used in PYCAP Analysis

Backfill Type	Moist Unit Weight (kN/m^3)	Friction Angle ϕ (°)	Wall Friction Angle δ (°)	Initial Soil Modulus E_i (kN/m^2)	3D Adjustment Factor (R_d)	Deflection at Failure Δ_{max}/H
Silty Sand	17.3	27.7	20.8	9600	1.18	0.05
Gravel	22.15	42.6	32	48,900	1.46	0.05